Journal of
Nanoscience and Nanotechnology
Vol. 10, 1461–1472, 2010

III–V/Silicon-on-Insulator Nanophotonic Cavities for Optical Network-on-Chip*

Liu Liu*, Günther Roelkens, Joris Van Campenhout†, Joost Brouckaert, Dries Van Thourhout, and Roel Baets

Photonics Research Group, INTEC Department, Ghent University-IMEC, St-Pietersnieuwstraat 41, 9000 Gent, Belgium

We review some opto-electronic devices based on the III–V/SOI heterogeneous integration platform, including lasers, modulators, wavelength converters, and photo-detectors. All of them are critical components for future on-chip interconnect and optical network-on-chip. The footprints of such devices are kept small by employing micro-cavity based structures. We give an overview of the device performances. The advantages over the all-silicon based devices are also discussed.

Keywords: Silicon Photonics, Silicon-on-Insulator, Microdisk Laser, Heterogeneous Integration, Optical Interconnect.

CONTENTS

1. Introduction 1461
2. III–V/SOI Die-to-Wafer Bonding 1463
3. Micro-Disk Laser 1464
4. Micro-Disk Modulator 1467
5. Wavelength Converter Based on a Micro-Disk Laser 1468
6. Wavelength-Selective Resonant Photo-Detector 1468
7. Heterogeneous III–V/SOI Micro-Cavity 1469
8. Conclusions 1470
Acknowledgment 1471
References and Notes 1471

1. INTRODUCTION

The interconnect bottleneck is envisioned as one of the critical challenges in the progress of integrated electronic circuits.[1] As the size of the gate length scales down, the speed and cost of an individual logic element improve, but unfortunately the performance of electric interconnect gets worse due to the resistive nature of metal wires. The response time (related to the resistance–capacitance product) and the power consumption (including dynamic capacitive load and Joule heat) of such a interconnect wire increases as the linewidth shrinks.[2] This places a limitation to the overall data-processing performance even on the chip level.[3,4] Optical interconnect is considered as a solution to this bottleneck. By replacing the electric wires with low-loss optical waveguides,[5,6] the energy dissipation in the connection wire itself can be reduced to a negligible level. Furthermore, an optical waveguide can provide virtually unlimited bandwidth for data communication, although the wavelength-division-multiplexing (WDM) technique might be necessary to fully exploit it.[7–9] Due to these promising perspectives, more and more research interests have been attracted to on-chip optical interconnect on both architectural designs and enabling technologies. In recent years, the idea of optical network-on-chip (ONoC) has also been introduced, where interconnect networks with more sophisticated routing and switching abilities within the optical domain—rather than the basic point-to-point links—were involved.[10–13]

Due to the compatible fabrication processes with complementary metal oxide semiconductor (CMOS) technology, silicon is probably the most suitable material to accommodate optical interconnect with the integration of electronic circuits. This advantage can largely improve the yield, reproducibility, and cost. Particularly, on the silicon-on-insulator (SOI) platform, the dimension of a single mode waveguide can be shrunk to, e.g., 500×220 nm^2, and the propagation loss of it can be less than 1 dB/cm.[6] This sub-micron sized waveguide leads to high-density integration of devices, which further reduces the cost. However, the full electronic–photonic integration based on silicon is still hampered by the absence of a compact and efficient light source, due to the indirect band-gap of silicon. Researchers have introduced various strategies to achieve all-silicon based lasers,[14–17] but they are still struggling for the efficiency and the feasibility of high-density integration. III–V compound semiconductors

*Author to whom correspondence should be addressed.
†Currently with IBM T. J. Watson Research Center, 1101 Kitchawan Rd., Yorktown Heights, NY 10598, USA.
*This is an invited review paper.

Liu Liu received the B. Eng. in Information Engineering in 2002 at Zhejiang University, China, and Ph.D. in Photonics in 2006 at the Royal Institute of Technology (KTH), Sweden. He joined Photonics Research Group, Department of Information Technology (INTEC), Ghent University, Belgium, as a post doctoral researcher from 2007 to 2009. Now he is with Department of Photonics Engineering, Technical University of Denmark, DTU–Fotonik, Denmark. His current research area is heterogeneous integration, and silicon nanophotonic devices.

Günther Roelkens (S'02-M'07) received the electronic engineering degree in 2002 and the Ph.D. degree in 2007 from Ghent University, Ghent, Belgium. Since 2002, he has been with the Department of Information Technology, Ghent University-Interuniversity Microelectronics Center (IMEC). Since 2007 he is working as a post-doc in the Photonics Research Group of Ghent University/IMEC. He is also an assistant professor in the Opto-electronic devices group at the Technical University of Eindhoven. His research interests are high efficiency interfaces between optical fiber and photonic integrated circuits and the heterogeneous integration of III–V semiconductors on top of silicon-on-insulator photonic integrated circuits.

Joris Van Campenhout received a Masters degree in Engineering Physics from Ghent University in 2002. In 2007, he was awarded the Ph.D. degree in Electrical Engineering from the same institution, for his work on electrically injected micro-disk lasers on a heterogeneous InP-Si platform. Dr. Joris Van Campenhout joined the IBM Thomas J. Watson Research Center in Yorktown Heights, NY in September 2007 as a Postdoctoral Scientist. He is currently working on electro-optic and thermo-optic devices for low-power switching in on-chip optical networks.

Joost Brouckaert received the electronic engineering degree from Ghent University, Gent, Belgium, in 2004. Since 2004, he has been with the Photonics Research Group, Department of Information Technology, Ghent University, Interuniversity Microelectronics Center. He is currently working towards his Ph.D. in the field of heterogeneous integration and silicon-on-insulator nanophotonic components.

Dries Van Thourhout (S'99–M'00) received the physical engineering degree and the Ph.D. degree from Ghent University, Gent, Belgium, in 1995 and 2000, respectively. He was with Lucent Technologies, Bell Laboratories, Crawford Hill, NJ, from October 2000 to September 2002, working on the design, processing, and characterization of InP/InGaAsP monolithically integrated devices. In October 2002, he joined the Photonics Research Group, Department of Information Technology, Ghent University, Interuniversity Microelectronics Center, continuing his work on integrated optoelectronic devices. His main interests are heterogeneous integration by wafer bonding, intrachip optical interconnect, and wavelength-division-multiplexing devices.

Roel Baets (M'88–SM'96) received the electrical engineering degree from Ghent University, Gent, Belgium, in 1980, the M.Sc. degree in electrical engineering from Stanford University, Stanford, CA, in 1981, and the Ph.D. degree from Ghent University, in 1984. He joined the Department of Information Technology (INTEC), Ghent University in 1981, and since 1989, he has been a Professor in the Engineering Faculty. From 1990 to 1994, he has also been a Part-Time Professor at the Technical University of Delft, Delft, The Netherlands. He has mainly worked in the field of photonic components. With about 300 publications and conference papers as well as about ten patents, he has made contributions to the design and fabrication of III–V semiconductor laser diodes, passive guided-wave devices, photonic integrated circuits, and microoptic components. He currently leads the Photonics Research Group, INTEC, Ghent University, which is an associated laboratory of the Interuniversity Microelectronics Center, working on integrated photonic devices for optical communication, optical interconnect, and optical sensing. Dr. Baets is a member of the Optical Society of America; the IEEE Lasers and Electro-Optics Society, where he was formerly a Chairman of the Benelux Chapter from 1999 to 2001 and is currently a member of the Board of Governors; the International Society for Optical Engineers; and the Flemish Engineers Association. He has been a member of the program committees of the Optical Fiber Communications Conference, the European Conference on Optical Communication, the IEEE Semiconductor Laser Conference, European Solid-State Device Research Conference, the Conference on Lasers and Electro-Optics—Europe, and the European Conference on Integrated Optics.

provide superior performance for light emission, and they also outperform silicon in some other aspects, e.g., high nonlinearity, high speed, efficient light detection at infrared wavelengths, etc. However, the drawbacks of III–V materials are their large device footprint and high cost. Heterogeneous integration of SOI and III–V, which combines the advantages of both materials, is therefore considered to be an efficient and complete platform for on-chip optical interconnect in the near future.

There are three main approaches for the integration of III–V material and silicon, which are flip-chip integration, hetero-epitaxial growth, and bonding technology. Flip-chip is the most matured technique, in which the finished optoelectronic components or chips are flipped over and bonded on the SOI circuit through soldering.[18] This sort of package-level integration is time-consuming and also less dense, since each of the chips has to be aligned and bonded sequentially. Hetero-epitaxial growth of III–V on silicon, on the other hand, offers the potential of dense integration. However, the lattice mismatch between the two materials results in a high density of crystal defects, and degrades the device performance significantly.[19] Bonding technology allows the integration of a high-quality III–V thin film onto the SOI structure.[20, 21] The III–V film is unpatterned initially and the devices in it are fabricated after the bonding process with, e.g., the standard CMOS technology, which can provide high alignment accuracy, high yield, and high integration density. The III–V/SOI die-to-wafer bonding is adopted in this paper, and will be described in detail in the next section. We will also review our recent results of micro-cavity based devices fabricated through the bonding technology, including micro-disk lasers (MDLs), micro-disk modulators, wavelength convertors, and resonant photo-detectors,[22–25] which are all critical components for on-chip optical interconnect and ONoC. A novel type of heterogeneous III–V/SOI cavity for light emission and nonlinearity enhancement will be discussed as well.[26]

2. III–V/SOI DIE-TO-WAFER BONDING

Figure 1 shows the processing flow of the device fabrication based on the III–V/SOI die-to-wafer bonding. Generally, III–V dice with appropriate sizes are first bonded up side down on top of the processed SOI wafer. Dice with different III–V layer structures can be bonded on the same SOI wafer. Since these III–V dice are unpatterned at this stage, only a coarse alignment is needed to just ensure they cover the areas where the active components will be located. Then, the InP substrate is removed by mechanical grinding and chemical etching. To isolate the etching solution from the target III–V layers, an etch stop layer

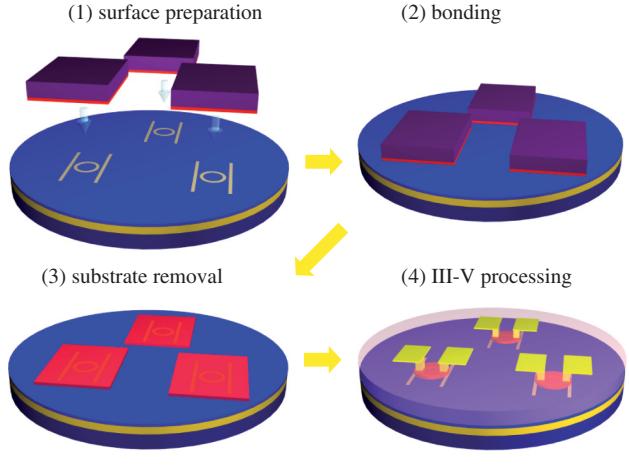

Fig. 1. Processing flow of the device fabrication with the III–V/SOI die-to-wafer bonding technology.

(usually InGaAs), which will be removed subsequently, is embedded between these layers and the substrate. The devices in the bonded III–V layers are then lithographically aligned and fabricated with standard wafer-scale processing.

To achieve a reliable bonding between the III–V dice and the SOI wafer, two techniques have been introduced, namely, SiO_2 molecular bonding[20] and benzocyclobutene (BCB) adhesive bonding[21] as sketched in Figure 2. In the first approach, the SOI wafer is covered by a SiO_2 layer, and then planarized by chemical mechanical polishing (CMP). A thin SiO_2 layer is also deposited on the III–V die. Subsequently, these two SiO_2 surfaces are chemically activated and then brought in contact. After an annealing process, the III–V die and the SOI wafer are bonded together by the van der Waals force. Both surfaces must be particle-free and the roughness has to be within a few atomic layers, so that the van der Waals attraction can take place in a large portion of the bonded surfaces. In the adhesive bonding approach, a polymer film (e.g., BCB) is first spin-coated on the SOI wafer. Due to the liquid form of the BCB solution, the topography of the SOI wafer can be planarized, and some particles, at least with diameters smaller than the BCB layer thickness, are acceptable. After applying the BCB film, the SOI wafer is baked at 150 °C for a short time to drive out the solvent, and the III–V die is attached on top. The whole stack is then cured in an oven at 250 °C for one hour to polymerize the BCB completely. Obviously, BCB adhesive bonding technology is more tolerant to the cleanliness of the fabrication environment and the quality of the bonded surfaces. Bonding by means of thick BCB layers (several hundred nanometers or more) is simple and reliable. As a comparison, the yield of the SiO_2 molecular bonding is only about 50%. On the other hand, due to the fluidity of the BCB material before curing and the uncontrolled pressure applied on the dice in the current bonding method, the uniformity of the BCB thickness is poor, which can vary several tens of nanometer within the same chip and about 100 nm from chip to chip. Through a dedicated bonding equipment with a well-controlled, uniform, and constant pressure during the curing process, the uniformity of the BCB thickness within 10% should be achievable. The thinner the bonding layer becomes, the more demanding the bonding process is. Recently, we have successfully achieved a BCB bonding layer thickness (defined as the distance between the top of the SOI waveguide and the bottom of the III–V layer) of about 50 nm.[26] This opens up the possibilities for some new applications, e.g., a heterogeneous III–V/SOI structure with an ultra-thin III–V overlay,[26] which will be discussed later. Both the SiO_2 molecular bonding and BCB adhesive bonding were employed for fabricating the devices in this paper.

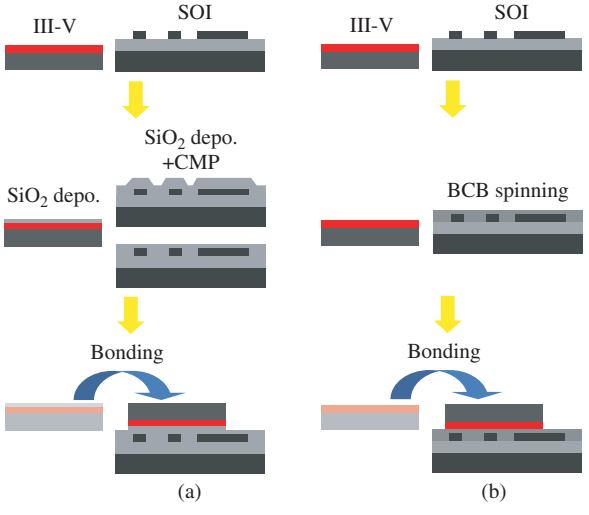

Fig. 2. Sketch of (a) the SiO_2 molecular bonding and (b) the BCB adhesive bonding processing.

3. MICRO-DISK LASER

Electrically-pumped Fabry-Perot (FP) lasers, distributed feed-back (DFB) lasers, and distributed Bragg reflector (DBR) lasers with lengths of several hundred microns have been recently demonstrated by using the III–V/SOI bonding technology.[27–29] To further reduce the footprint of the laser device, we employed a micro-disk structure, as shown in Figure 3, which is fabricated through SiO_2 molecular bonding.[22] The III–V disk typically has a diameter of about 10 μm, and thickness of 1 μm in order to accommodate the *p–i–n* junction for electrical pumping.

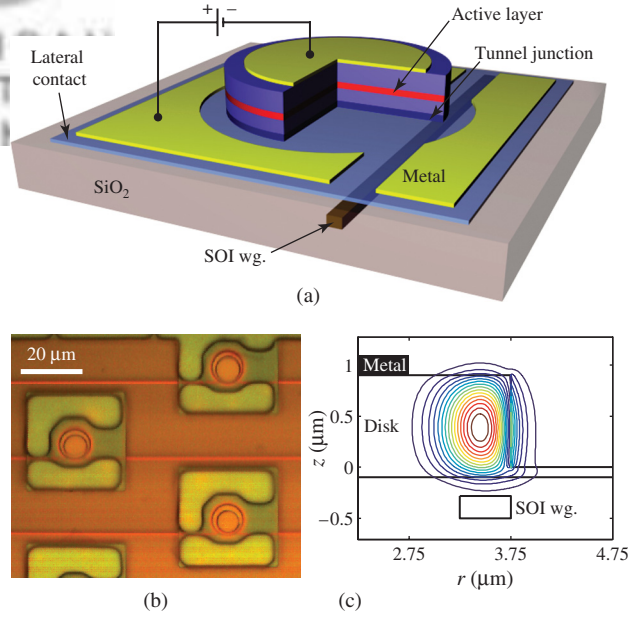

Fig. 3. (a) Structure of the MDL integrated on an SOI waveguide. (b) Microscope picture of fabricated devices before metallization. (c) E_r-field amplitude distribution of the fundamental WGM in a micro-disk with 7.5 μm diameter.

The resonant mode is the whispering gallery mode (WGM) confined at the periphery of the disk. Figure 3(c) shows the E_r field distribution of the fundamental WGM. The optical gain is provided by three compressively strained quantum wells embedded in the middle of the III–V layer. Laser light is coupled out by the evanescent coupling to the underlying SOI waveguide aligned to the edge of the disk. The SiO_2 bonding layer thickness is typically 100 nm–200 nm. The top metal contact is positioned at the center of the disk, where the mode field is nearly zero. The bottom contact is deposited on a thin lateral contact layer of about 100 nm thick. A reverse biased tunnel junction is located above this lateral contact layer for hole injection. As compared to conventional *p*-type contacts, this tunnel-junction based contact provides a low optical loss, a low contact resistance, and also a uniform current distribution in the whole disk area.[30] We refer to Ref. [22] for the III–V epitaxial layer and the detailed fabrication processes.

Figure 4 shows the lasing characteristics of an MDL with 10 μm diameter under continuous driving conditions. Due to the small size, the free spectral range (FSR) of the cavity resonance (i.e., the wavelength difference of the two adjacent azimuthal modes) is large (24 nm in this case). Thus, single-mode lasing was obtained as shown in Figure 4(a). The side-mode suppression ration is about 22 dB. The light–current–voltage (LIV) relation of the MDL is plotted in Figure 4(b). The threshold current is 1.0 mA, which corresponds to a current density of 1.27 kA/cm^2, assuming uniform injection. One can see that the lasing powers measured at the two ends of the SOI waveguide are approximately equal. This means that the MDL actually works in the bi-directional regime,[31] where the clockwise and the counter-clockwise propagations of the WGM coexist. The peak lasing power in the SOI waveguide is about 10 μW limited by the early thermal rollover, since the thermal resistance of the device is high (measured to be 4.8 K/mW) due to the relatively thick SiO_2 buffer layer (1 μm).[32] The sudden drop of the power beyond 5 mA is due to the switching of the lasing mode to another azimuthal order with a longer wavelength, since the peak gain wavelength of the quantum wells red-shifts at an elevated temperature. The long and short range oscillations of the light–current curves above threshold are most likely due to the reflection feedback (calculated to be about −22 dB) from the grating couplers used for interfacing between the SOI waveguide and the single mode fiber.[33] Continuous lasing operation was also obtained for micro-disks of 7.5 μm diameter with similar characteristics. However, No lasing was achieved with 5 μm diameter disks probably due to the relatively large misalignment of the top metal contact resulted from the contact lithography. More advanced lithography tools, e.g., a high-end deep-ultraviolet (DUV) stepper, might be necessary for obtaining a working MDL of such a small size.

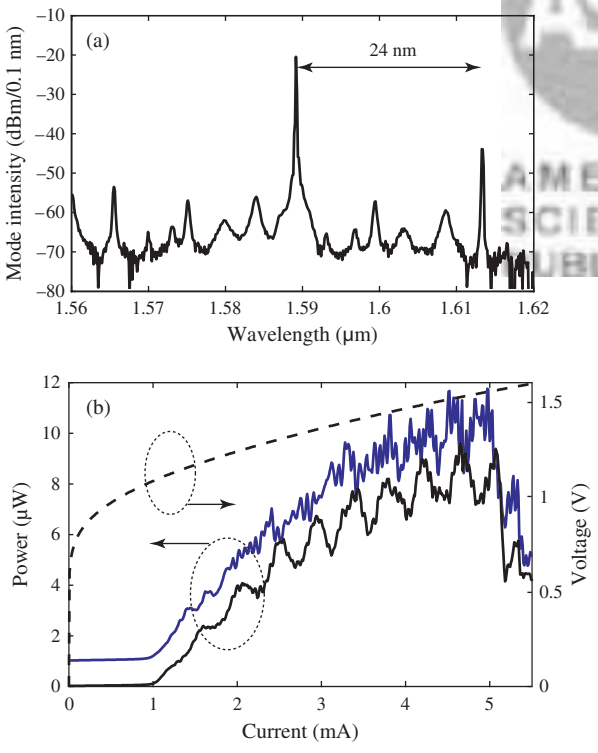

Fig. 4. (a) Lasing spectrum of a 10 μm MDL at a bias of 4.8 mA. (b) LIV curves of the same laser. The dashed line indicates the voltage; the solid lines indicate the powers towards the two ends of the SOI waveguide. The blue solid line is offset by 1 μW for clarity.

The dynamic response of an MDL is an important characteristic, as the direct modulation of the bias current is the easiest and most compact way to imprint a data pattern onto the laser beam. Figure 5(a) shows the typical small signal modulation response of a 7.5 μm diameter MDL. The 3 dB bandwidth is about 3.5 GHz. The large signal modulation response is also plotted in Figure 5(b), where the MDL was modulated with a periodic square-wave signal at 1.5 GHz (3.0 Gbps). Here, the low level of the driving signal was slightly above threshold, and the high level was at the current giving the highest power. No significant overshoot is observed. The extinction ratio of the optical signal is 10 dB after the amplification by an Er-doped fiber amplifier (EDFA). The rise and fall time is 110 ps and 150 ps, respectively. The eye-diagram analysis reveals that the data transmission performance is actually limited by the low signal-to-noise ratio resulted from the relatively weak lasing power (e.g., 10 μW) obtained so far. Simulation shows that the output power can be increased by at least an order of magnitude with an optimized structure.[34] This will improve significantly the signal-to-noise ratio, as well as the operation speed.

As we mentioned above, WDM might be a necessary technology for ONoC, where information is carried on different wavelengths but transferred in one waveguide. For this purpose, a multi-wavelength laser is required, and it can be readily realized by cascading several MDLs with

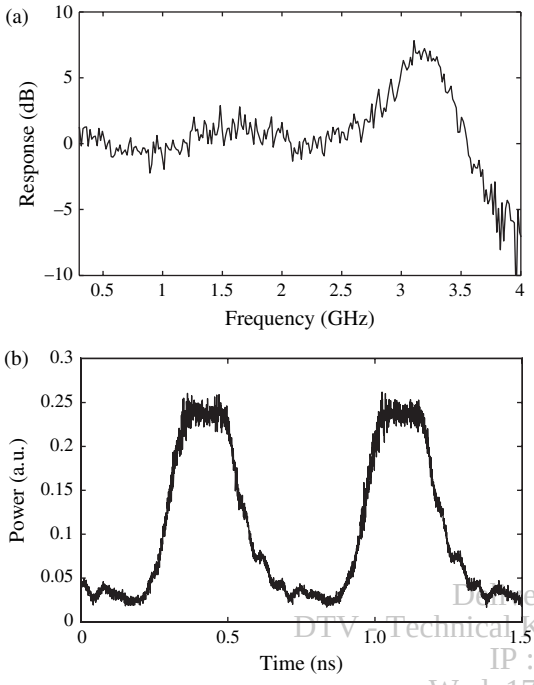

Fig. 5. (a) Small signal modulation response of a 7.5 μm-diameter MDL. (b) Large signal modulation response of the same laser with an electrical driving signal of a periodic square-wave at 1.5 GHz.

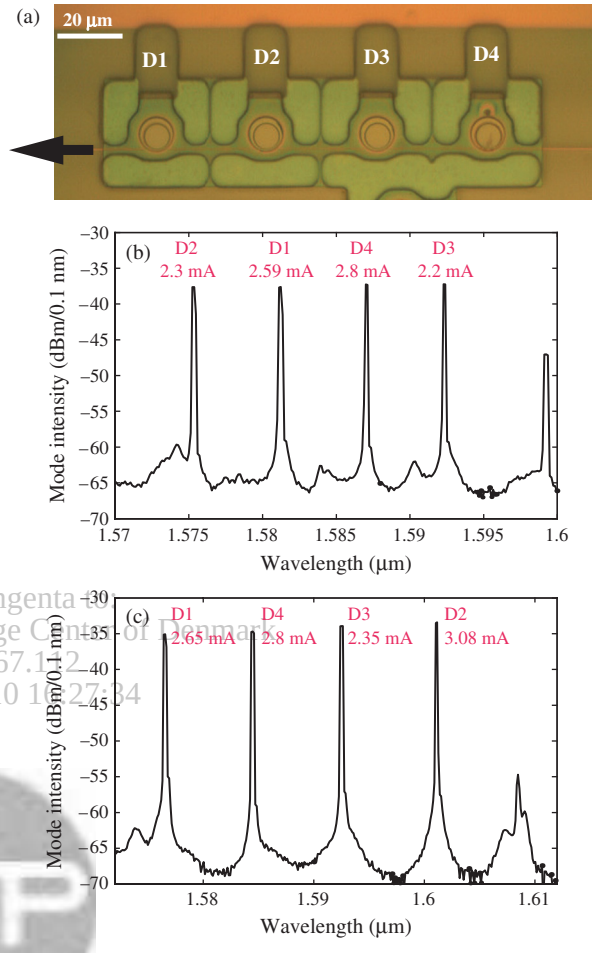

Fig. 6. (a) Fabricated multiwavelength laser before metallization, composed of four MDLs on one bus SOI waveguide. Arrow indicates the monitoring direction. Spectra of two multiwavelength lasers with (b) 6 nm channel spacing and (c) 8 nm channel spacing. The bias current of each MDL is marked on the corresponding lasing peak. (a) and (c) are Reprinted with permission from [23], J. Van Campenhout et al., *IEEE Photon. Technol. Lett.* 20, 1345 **(2008)**. © 2008, IEEE.

slightly different diameters on one bus SOI waveguide, as shown in Figure 6(a).[23] This simple configuration is favored by the evanescent out-coupling scheme of an MDL, whereas for a conventional FP, DFB, or DBR laser a multiplexer has to be included for the same functionality.[27–29] We present in Figures 6(b and c) the measured spectra of two 4-channel multi-wavelength lasers: one for 6 nm channel spacing, the other for 8 nm channel spacing. To achieve a uniform emitting power, the bias current of each MDL has been adjusted individually. This is mainly due to the insertion loss caused by one micro-disk. The 1 μm thick III–V layer supports several high-order modes in the vertical direction. When the laser light from one MDL passes through the adjacent micro-disks to the output port, part of the power will be lost due to the coupling to these high-order modes. Measurements show that this insertion loss is about 3 dB.[23] For this reason, the emitting powers of all the other MDLs have to compromise with that of the MDL the most distant to the output port through, e.g., adjusting their bias currents. This approach might become unrealistic, if a large number of channels are involved. An alternative solution to this problem is to decrease the III–V layer thickness (e.g., to about 300 nm) so that single mode operation is ensured in the vertical direction. Numerical simulations suggest that 0.1 dB insertion loss can be achieved with this approach. However, designing an efficient *p–i–n* structure in this ultra-thin III–V layer, while keeping a reasonable optical loss is still challenging. Another reason for the power non-uniformity comes from the wavelength dependence of the material gain, which can be minimized by reducing the channel spacing. Due to the fabrication accuracy, the lasing wavelengths of identical micro-disks vary about ±500 pm in the same chip. Therefore, a trimming mechanism, e.g., a local heater, would be necessary to align each of the lasing peaks to the desired channel grid.

Although the MDLs mentioned above are all based on the SiO_2 molecular bonding, BCB bonding technology has also been employed recently. Since BCB ($n = 1.54$) has a slightly higher refractive index as compared to SiO_2 ($n = 1.44$), the coupling efficiency to the SOI waveguide is expected to be larger, likely resulting in a higher output power. On the other hand, the thermal conductivity of BCB (0.3 W/mK) is lower than that of SiO_2 (1.2 W/mK), so the thermal resistance of the whole device would be also larger, which limits the amount of current that can be applied. Similar performances have been obtained with BCB-bonded MDLs. Figure 7 shows the lasing spectrum

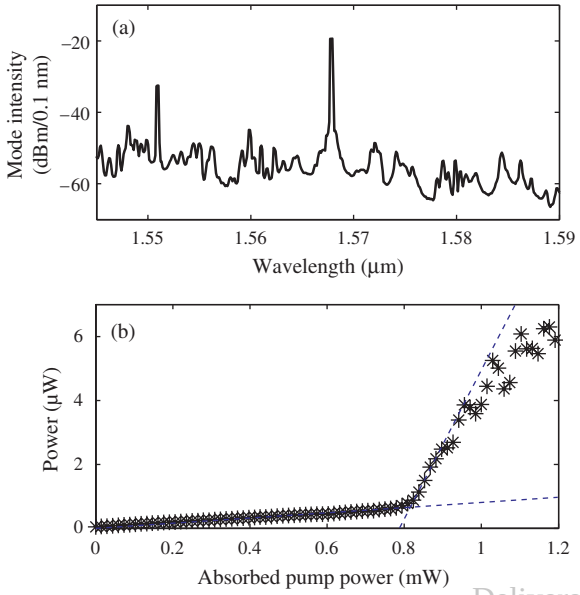

Fig. 7. Lasing characteristics of a BCB-bonded MDL with 15 μm diameter. (a) Lasing spectrum; (b) Lasing power as a function of the absorbed pump power. The optical pump source is a 980 nm laser diode.

and power response of a BCB-bonded MDL with 15 μm diameter under optical pumping.

4. MICRO-DISK MODULATOR

Instead of using MDLs as on-chip light sources, an external laser might be employed for stronger power or better performance. This laser beam will be coupled to and shared by the whole chip. Local electro-optic modulators are therefore needed to place the information on the carrier laser beams. There have been lots of reports on all-silicon based modulators mainly through two approaches: carrier depletion[35, 36] or carrier injection.[37–40] Both of them rely on the free carrier dispersion (FCD) effect, i.e., the refractive index of silicon varies with different carrier concentrations.[41] A Mach-Zehnder interferometer structure is commonly used to translate the phase modulation to the intensity modulation.[35, 40] Alternatively, a ring or disk resonant cavity can also be employed, which helps to reduce the device size and the power consumption, but the operational wavelength range is confined only around the resonant wavelengths.[37–39]

Recently, various heterogeneously-integrated modulators have been demonstrated by using GeSi material[42] or III–V quantum wells.[43, 44] We also proposed a III–V micro-disk modulator integrated on an SOI waveguide.[24] The structure is essentially the same as the MDL introduced above (cf., Fig. 3). The working principle relies on the modulation of the loss or gain of the active layer in the micro-disk cavity via current injection.[45] Figure 8(a) shows the static transmission spectra of transverse-electric (TE) polarized light in the SOI waveguide. At zero bias, no

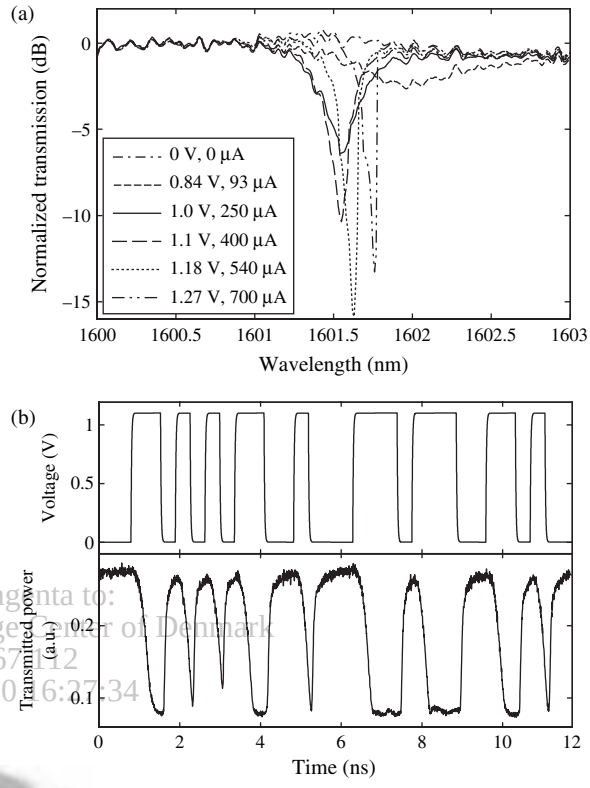

Fig. 8. (a) Normalized transmission spectrum of the micro-disk modulator at different biases. (b) Electric driving signal and corresponding optical response of the micro-disk modulator at 2.73 Gbps. Reprinted with permission from [24], L. Liu et al., *Opt. Lett.* 33, 2518 **(2008)**. © 2008, Optical Society of America.

resonant dip is observed. This is due to the fact that the intrinsic loss of the micro-disk cavity (mainly from the large band-to-band absorption of the active layer) is much higher than that of the coupling loss to the SOI waveguide. The cavity works in an under-coupled regime. As the bias current increases, the absorption of the active layer is compensated by the injected carriers, and even gain can be obtained. The resonant dip also becomes more and more obvious, meaning that the micro-disk cavity approaches the critical-coupling point where the intrinsic loss and the coupling loss are equal. An extinction ratio of about 10 dB is obtained at 400 μA/1.1 V bias which is further confirmed to be the best operation point of the present device, since at this current level the active layer in the cavity is likely at transparency which gives a power-independent modulation depth.[24] The shift of the resonant dip results from the competition between the FCD effect and the thermo-optic effect. At low currents, the former one dominates (blue-shift), and as the bias increases further the latter starts to take over (red-shift). The dynamic modulation results are shown in Figure 8(b), where the waveforms of the electric driving signal and the corresponding optical signal using a 32-bit non-return-zero (NRZ) pattern at a bit rate of 2.73 Gbps are presented. One can see the information was reversely transferred onto the laser beam.

The optical modulation depth is about 6 dB, slightly less than the static result (10 dB), due to the significant spontaneous emission from the EDFA employed to amplify the output signal. Note that we obtained this operation speed without using any special drive techniques, while <1 Gbps NRZ modulation was originally reported in the carrier-injection based silicon modulators due to the slower carrier dynamics.[37, 38] The speed of those devices has been pushed to about 10 Gbps with the pre-emphasis technique,[39, 40] and this approach can also be employed to the proposed device. The dynamic power consumption of the present modulator is estimated to be about 250 fJ/bit, which is less than those of the carrier-injection based silicon modulators (300–5000 fJ/bit),[39, 40, 42] but still high as compared to some carrier-depletion or electro-absorption (EA) based modulators (tens of fJ/bit).[36, 42, 43] The power consumption can be reduced, to some extent, by creating a central hole, or employing an ultra-small disk. Besides through carrier injection as demonstrated here, the loss of an III–V active layer can also be modified via, e.g., the EA effect under a reverse bias.[43] This can largely reduce the power consumption, and also improve the operation speed.

5. WAVELENGTH CONVERTER BASED ON A MICRO-DISK LASER

Wavelength conversion plays an important role in WDM telecommunication networks, which enables the dynamic allocation of the limited wavelength resources.[46] In future ONoC, an all-optical wavelength convertor might also be a useful element. Based on silicon, the four-wave mixing (FWM) effect[47, 49] or the FCD effect accompanied by two-photon absorption (TPA)[48] have been employed for realizing such a device. Since FWM and TPA are all high-order nonlinear effects of silicon (based on $\chi^{(3)}$: the third-order susceptibility),[50] a strong optical signal is required. By employing an SOI wire waveguide with a tightly-confined optical field and a ring resonant cavity, the power of the control signal has already been reduced to several milliwatts.[49] However, since it is not so straightforward to build an integrated optical amplifier on SOI, this power level might be still too high for applications like ONoC.

By using the MDLs, ultra-low-power wavelength conversion has been achieved.[25] Figure 9(a) shows our experimental setup. For wavelength conversion, an external control laser of TE polarization was injected to the MDL through the SOI waveguide. This laser beam was tuned to the wavelength of the second highest spectral peak of the laser, which is one FSR away from the natural lasing peak at the longer wavelength side (another azimuthal order). The output light was pre-amplified. A band-pass filter was used to block the residual control signal, and only the natural lasing wavelength of the MDL was detected. Figure 9(b) shows the static lasing spectra with and without an injected light. One can find that the information carried on the injected signal could be imprinted to the natural

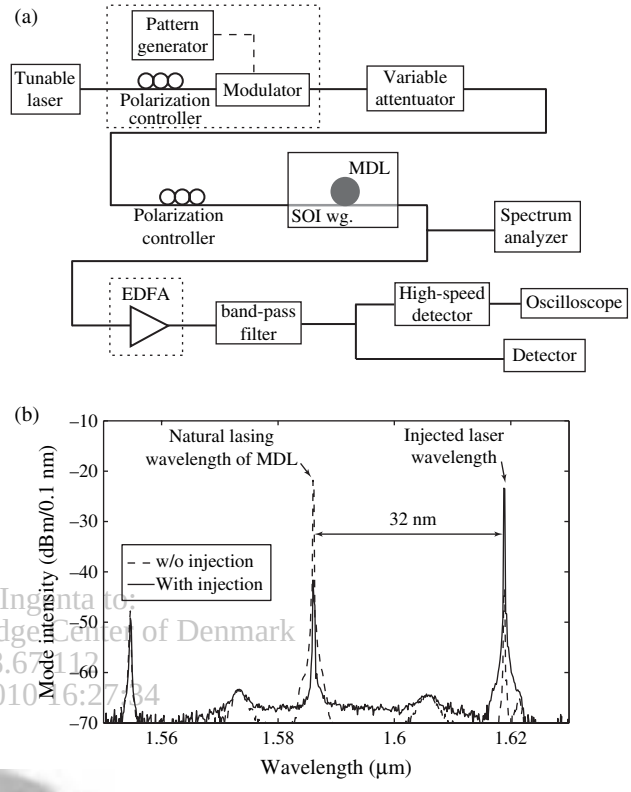

Fig. 9. (a) Measurement setup for wavelength conversion. The equipments in the dotted frames were added for dynamic measurements. (b) Measured spectra with and without an injected laser, showing the working principle of the wavelength converter.

lasing light of the MDL in a reversed way. Figure 10(a) shows the measured natural lasing power as a function of the injected wavelengths. A clear dip can be observed when the injected beam is at resonance with the cavity mode around 1620 nm (cf., Fig. 9(b)). 6.4 μW injected power suffices to achieve about 20 dB extinction ratio of the converted signal. Such a low control power is obtained by the gain provided by the active material in the micro-disk cavity. The dynamic wavelength conversion is shown in Figure 10(b) where the input control signal is a 5 Gbps NRZ code with 2^{31}-1 pseudo random bit sequence. Although an open eye was obtained, the performance is still limited by the low signal-to-noise ratio of the natural lasing as we mentioned above.

6. WAVELENGTH-SELECTIVE RESONANT PHOTO-DETECTOR

Single crystalline silicon shows low absorption losses for guiding infrared light.[5, 6] This implies that it is not a good candidate for light detection at these wavelengths. Commonly, silicon can be made absorbing by the incorporation of doping elements, e.g., Erbium,[51] or the introduction of the crystal defects through, e.g., proton implantation.[52] It has been shown that photocurrent can also been generated through TPA in silicon.[53]

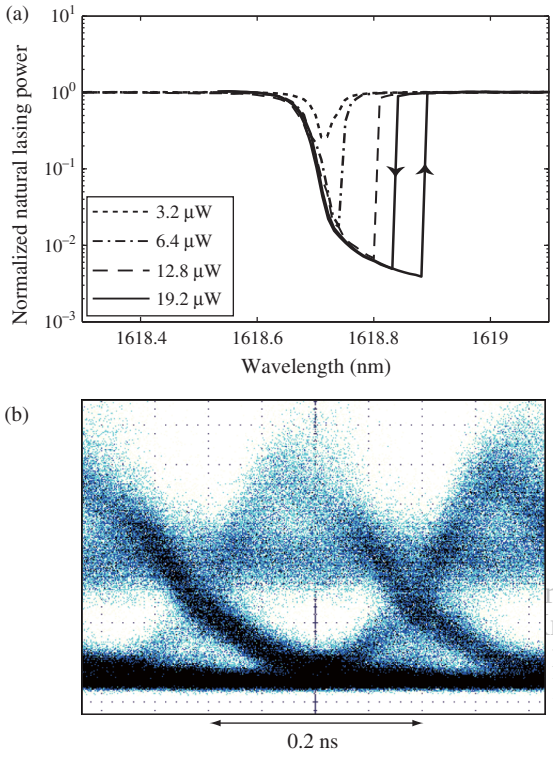

Fig. 10. (a) Power at the natural lasing wavelength as a function of the injected wavelength. (b) Eye diagram of the converted signal as the injected laser was modulated at 5 Gbps. Reprinted with permission from [25], L. Liu et al., *Appl. Phys. Lett.* 93, 061107 (**2008**). © 2008, American Institute of Physics.

However, these all-silicon based infrared detectors still have very low efficiency, and are outperformed by their counterparts based on, e.g., InGaAs. We have introduced an evanescently-coupled, InGaAs/InAlAs metal–semiconductor–metal (MSM) photo-detector integrated on an SOI waveguide through the BCB adhesive bonding.[54] Figure 11(a) shows a schematic cross section of such a detector. Responsivity of 1.0 A/W at a broad wavelength

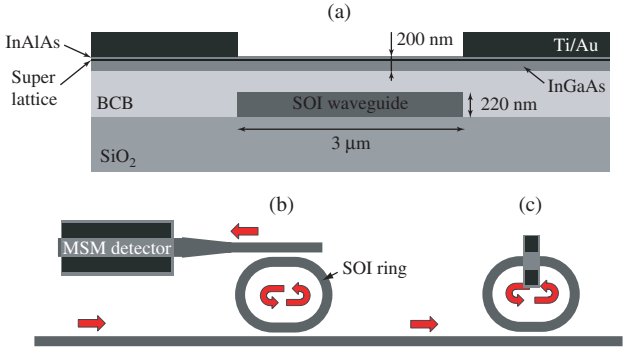

Fig. 11. (a) Cross-sectional sketch of the InAlAs/InGaAs MSM detector on an SOI waveguide. The input light is in the SOI waveguide travelling perpendicularly to the paper plane. (b) Conventional configuration of a wavelength-selective detector based on an SOI ring cavity; (c) Proposed configuration with the III–V absorption layer bonded on top of the ring.

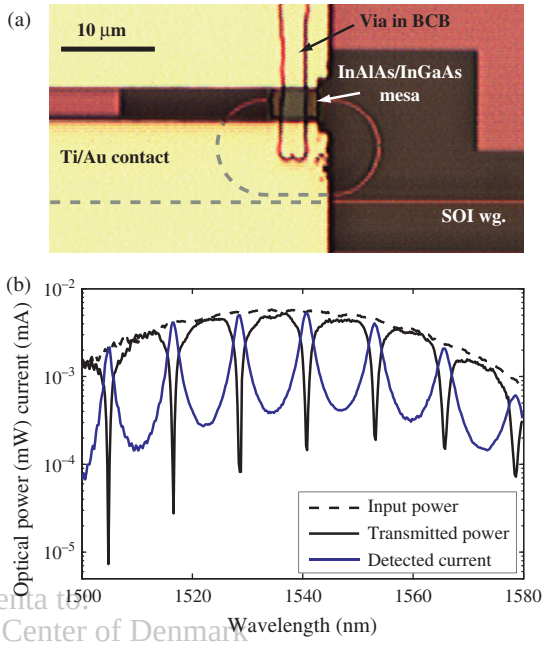

Fig. 12. (a) Microscope picture of a fabricated device. (b) Transmitted power and detected current as a function of the input laser wavelength.

range has been demonstrated with a detector length of 25 μm.[54]

In this paper, we propose a wavelength-selective resonant detector structure based on an SOI ring, which can be potentially used for ONoC involving WDM. Instead of using an SOI waveguide to lead the dropped light to the broadband MSM detector (see Fig. 11(b)), the InGaAs absorption layer is directly integrated on part of the SOI ring resonator in the proposed structure (see Fig. 11(c)). Therefore, the length of the detector can be further reduced (5 μm in the fabricated device shown in Fig. 12(a)). Figure 12(b) shows the measured responses under static conditions. A grating coupler was used to interface with an optical fiber, resulting in a Gaussian coupling spectrum.[33] One can see that the present detector only responds to the resonant wavelengths and the peak responsivity reaches 1.0 A/W. Off resonance, the detected current drops by more than 10 dB. At the through port of the SOI waveguide, the extinction ratio is also more than 10 dB. The dark current was measured to be around 0.5 nA, which is less than that of the originally broadband detector (5 nA) due to the smaller device area.

7. HETEROGENEOUS III–V/SOI MICRO-CAVITY

The devices discussed above are all based on the evanescent coupling between the SOI waveguide and the III–V layer, where guiding structures are defined in both materials (e.g., the SOI waveguide and the III–V micro-disks). Recently, we introduced a novel heterogeneous III–V/SOI structure, which consists of an SOI waveguide and a

bonded thin III–V film (sub 100 nm) using a very thin (i.e., 65 nm) BCB layer as shown in Figure 13(a). In this device configuration the optical mode is a hybrid mode which is predominantly confined in the SOI waveguide, but the tail of the mode overlaps with the III–V layer structure (see Figs. 13(b and c)). This allows using, e.g., DUV lithography to define the waveguide structures in the SOI layer, while keeping the III–V processing simple and less critical. Stimulated emission and strong nonlinear behavior in this hybrid waveguide structure can be achieved due to the overlap of the mode with the bonded III–V layer. A similar structure has also been employed in the molecular bonding technology for realizing lasers.[27–29] However, the weak optical confinement provided by different compositions of the III–V materials in the vertical direction leads to a large cross section of the underlying SOI waveguide, which does not allow sharp bends. In our structure, a strong confinement in the vertical direction is kept by employing a sub-100 nm thick III–V layer, and a single-mode SOI waveguide can therefore be adopted. Nonetheless, electrical pumping of these devices would be hard or probably impossible. Through optical pumping however, light emission can be realized as demonstrated in Figure 14, showing the emission spectrum from a ring cavity coupled to the SOI waveguide. While no lasing was obtained yet by pumping from the top of the III–V/SOI waveguide circuit due to the inefficient absorption of the pump light in the thin III–V layer, it is believed that lasing can be achieved with in-plane pumping using the SOI waveguide layer to route the pump light to the III–V/SOI cavity. This requires however dedicated resonator structures, which allow critical coupling for the pump wavelength and high quality factor for the lasing wavelength. Besides light emission, a strong nonlinear behavior was also observed which can

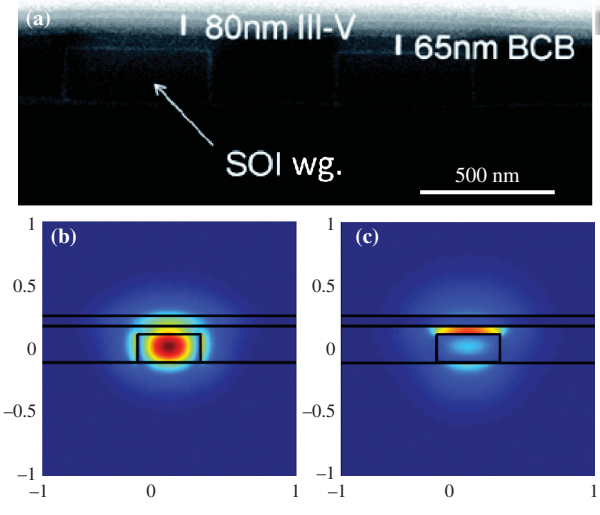

Fig. 13. (a) Cross-sectional picture of the heterogeneous III–V/SOI waveguide structure, showing an 80 nm III–V layer bonded on top of two SOI waveguides. Mode field distributions in this structure with (b) TE and (c) Transverse magnetic (TM) polarizations.

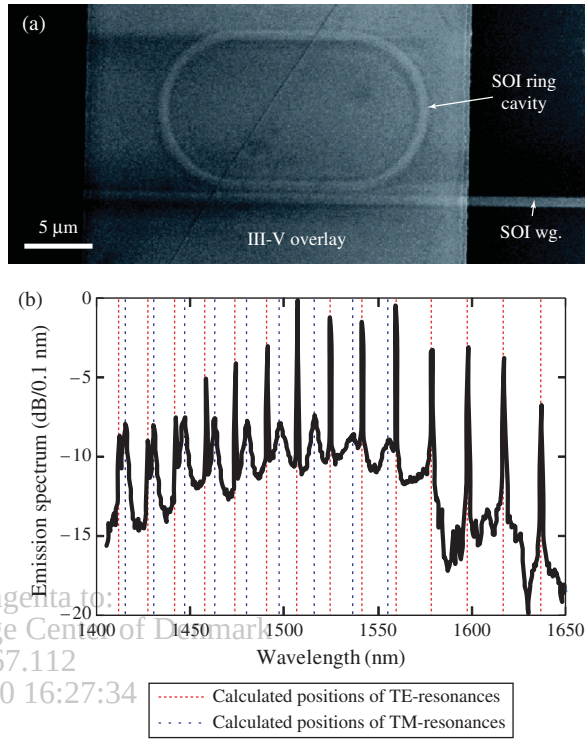

Fig. 14. (a) Scanning electron microscope picture of a heterogeneous III–V/SOI micro-cavity. (b) Emission spectrum coupled to the SOI waveguide under optical pumping. Reprinted with permission from [26], G. Roelkens et al., *J. Appl. Phys.* 104, 033117 **(2008)**. © 2008, American Institute of Physics.

be used for all-optical switching and wavelength conversion in an ONoC. This behavior results from the FCD effect of the III–V layer induced by the pump beam, which changes the resonance wavelength of the III–V/SOI cavity and thereby allows switching of a probe beam or imprinting of the pump beam data signal on a probe beam. Since the free carriers are generated through the direct band-to-band absorption, which is a much more efficient process as compared to the TPA adopted in all-silicon approaches,[48] better device performances, e.g., continuous wave operation, has been achieved.[26]

8. CONCLUSIONS

We have reviewed some basic opto-electronic components on silicon for future on-chip interconnect and ONoC, including lasers, modulators, wavelength converters, and photo-detectors. Heterogeneous integration of III–V materials and SOI structure through either SiO_2 molecular or BCB adhesive die-to-wafer bonding has been employed for realizing these components in a CMOS compatible way. This bonding technology combines the advantages of both materials, and provides an efficient and complete platform for on-chip interconnect and ONoC as discussed above. Micro-cavity based structures have been adopted for all the devices in this paper due to their compact size.

The performances of the fabricated devices based on the heterogeneous III–V/SOI platform have been studied and compared with their all-silicon based counterparts. Various advantages have been demonstrated, especially the efficient and compact laser sources which are still missing with all-silicon approaches. We also demonstrated III–V micro-disk modulators with 10 dB extinction ratio and 2.73 Gbps operation speed, wavelength converters with a control power as low as 6.4 μW, and compact wavelength-selective MSM photo-detectors. A heterogeneous III–V/SOI micro-cavity structure has been introduced, showing the potential for laser emission and nonlinear applications. Improving the performance of the individual components is one of our future objectives. This will enable a practical demonstration of an ONoC integrating all or part of the aforementioned devices together with the passive SOI circuits.

Acknowledgment: We acknowledge valuable assistances from Institut des Nanotechnologies de Lyon (France), CEA-LETI Minatec (France), TRACIT Technologies (France), OED Group, Technical University Eindhoven (The Netherlands), and Laboratoire de Photonique et de Nanostructures, CNRS (France). We would like to thank Dr. Richard A. Soref for fruitful discussions. We also thank Steven Verstuyft, Liesbet Van Landschoot, and Zon-Qiang Yu for part of the III–V processing. This work is partially supported by EU-funded projects WADIMOS, HISTORIC, and ePIXnet. L. Liu was supported by Interuniversity Attraction Poles (IAP) through a postdoctoral grant. G. Roelkens was supported by Scientific Research-Flanders (FWO) through a postdoctoral grant.

References and Notes

1. Z. Gaburro, Optical interconnect, Silicon Photonics, edited by L. Pavesi and D. J. Lockwood, Springer-Verlag, Berlin (**2004**), p. 121.
2. D. A. B. Miller, *Int. J. Optoelectron.* 11, 155 (**1997**).
3. M. Haurylau, G. Chen, H. Chen, J. Zhang, N. A. Nelson, D. H. Albonesi, E. G. Friedman, and P. M. Fauchet, *IEEE J. Sel. Topics Quantum Electron.* 12, 1699 (**2006**).
4. R. G. Beausoleil, P. J. Kuekes, G. S. Snider, W. Shih-Yuan, and R. S. Williams, *Proc. IEEE* 96, 230 (**2008**).
5. W. Bogaerts, R. Baets, P. Dumon, V. Wiaux, S. Beckx, D. Taillaert, B. Luysseart, J. Van Campenhout, P. Bienstman, and D. Van Thourhout, *J. Lightwave Technol.* 23, 401 (**2005**).
6. M. Gnan, S. Thorns, D. S. Macintyre, R. M. De La Rue, and M. Sorel, *Electron. Lett.* 44, 115 (**2008**).
7. T. Barwicz, H. Byun, F. Gan, C. W. Holzwarth, M. A. Popovic, P. T. Rakich, M. R. Watts, E. P. Ippen, F. X. Kärtner, H. I. Smith, J. S. Orcutt, R. J. Ram, V. Stojanovic, O. O. Olubuyide, J. L. Hoyt, S. Spector, M. Geis, M. Grein, T. Lyszczarz, and J. U. Yoon, *J. Opt. Netw.* 6, 63 (**2007**).
8. B. A. Small, B. G. Lee, K. Bergman, Q. Xu, and M. Lipson, *J. Opt. Netw.* 6, 112 (**2007**).
9. A. W. Poon, F. Xu, and X. Luo, *Proc. SPIE* 6898, 689812 (**2008**).
10. A. Shacham, K. Bergman, and L. P. Carloni, *Proc. 1st Intl. Symp. on Networks-on-Chip* (**2007**), pp. 53–64.
11. K. Bergman and L. Carloni, *Proc. SPIE* 6898, 689813 (**2008**).
12. R. G. Beausoleil, J. Ahn, N. Binkert, A. Davis, D. Fattal, M. Fiorentino, N. P. Jouppi, M. McLaren, C. M. Santori, R. S. Schreiber, S. M. Spillane, D. Vantrease, and Q. Xu, *IEEE LEOS Newsletter* 22, 15 (**2008**).
13. A. Scandurra and I. O'Connor, Scalable CMOS-compatible photonic routing topologies for versatile networks on chip, *Proc. 1st workshop on Network-on-Chip Architectures* (**2008**), pp. 44–50.
14. O. Boyraz and B. Jalali, *Opt. Express* 12, 5269 (**2004**).
15. H. S. Rong, R. Jones, A. S. Liu, O. Cohen, D. Hak, A. Fang, and M. J. Paniccia, *Nature* 433, 725 (**2005**).
16. L. Pavesi, L. Dal Negro, C. Mazzoleni, G. Franzò, and F. Priolo, *Nature* 408, 440 (**2000**).
17. S. Lombardo, S. Campisano, G. Vandenhoven, A. Cacciato, and A. Polman, *Appl. Phys. Lett.* 63, 1942 (**1993**).
18. T. Mitze, M. Schnarrenberger, L. Zimmermann, J. Bruns, F. Fidorra, J. Kreissl, K. Janiak, S. Fidorra, H. Heidrich, and K. Petermann, *Proc. 2nd IEEE Intl. Conf. on Group IV Photon* (**2005**), pp. 210–212.
19. D. Fehly, A. Schlachetzki, A. S. Bakin, A. Guttzeit, and H.-H. Wehmann, *IEEE J. Quantum Electron.* 37, 1246 (**2001**).
20. M. Kostrzewa, L. Di Cioccio, M. Zussy, J. C. Roussin, J.-M. Fedeli, N. Kernevez, P. Regreny, C. Lagahe-Blanchard, and B. Aspar, *Sens. Actuators, A: Physical* 125, 411 (**2006**).
21. G. Roelkens, J. Brouckaert, D. Van Thourhout, R. Baets, R. Notzel, and M. Smit, *J. Electrochem. Soc.* 153, G1015 (**2006**).
22. J. Van Campenhout, P. Rojo-Romeo, P. Regreny, C. Seassal, D. Van Thourhout, S. Verstuyft, L. Di Cioccio, J.-M. Fedeli, C. Lagahe, and R. Baets, *Opt. Express* 15, 6744 (**2007**).
23. J. Van Campenhout, L. Liu, P. Rojo-Romeo, D. Van Thourhout, C. Seassal, P. Regreny, L. Di Cioccio, J.-M. Fédéli, and R. Baets, *IEEE Photon. Technol. Lett.* 20, 1345 (**2008**).
24. L. Liu, J. Van Campenhout, G. Roelkens, R. A. Soref, D. Van Thourhout, P. Rojo-Romeo, P. Regreny, C. Seassal, J.-M. Fédéli, and R. Baets, *Opt. Lett.* 33, 2518 (**2008**).
25. L. Liu, J. Van Campenhout, G. Roelkens, D. Van Thourhout, P. Rojo-Romeo, P. Regreny, C. Seassal, J.-M. Fédéli, and R. Baets, *Appl. Phys. Lett.* 93, 061107 (**2008**).
26. G. Roelkens, L. Liu, D. Van Thourhout, R. Baets, R. Notzel, F. Raineri, I. Sagnes, G. Beaudoin, and R. Raj, *J. Appl. Phys.* 104, 033117 (**2008**).
27. A. W. Fang, H. Park, O. Cohen, R. Jones, M. J. Paniccia, and J. E. Bowers, *Opt. Express* 14, 9203 (**2006**).
28. A. W. Fang, E. Lively, Y.-H. Kuo, D. Liang, and J. E. Bowers, *Opt. Express* 16, 4413 (**2008**).
29. A. W. Fang, B. R. Koch, R. Jones, E. Lively, D. Liang, Y.-H. Kuo, and J. E. Bowers, *IEEE Photon. Technol. Lett.* 20, 1667 (**2008**).
30. S. Sekiguchi, T. Miyamoto, T. Kimura, G. Okazaki, F. Koyama, and K. Iga, *Jpn. J. Appl. Phys.* 39, 3997 (**2000**).
31. M. Sorel, G. Giuliani, A. Scire, R. Miglierina, S. Donati, and P. J. R. Laybourn, *IEEE J. Quantum Electron.* 39, 1187 (**2003**).
32. J. Van Campenhout, P. R. Romeo, D. Van Thourhout, C. Seassal, P. Regreny, L. Di Cioccio, J.-M. Fedeli, and R. Baets, *J. Lightwave Technol.* 25, 1543 (**2007**).
33. D. Taillaert, F. Van Laere, M. Ayre, W. Bogaerts, D. Van Thourhout, P. Bienstman, and R. Baets, *Jpn. J. Appl. Phys.* 45, 6071 (**2006**).
34. J. Van Campenhout, P. R. Romeo, D. Van Thourhout, C. Seassal, P. Regreny, L. Di Cioccio, J.-M. Fedeli, and R. Baets, *J. Lightwave Technol.* 26, 52 (**2008**).
35. A. Liu, L. Liao, D. Rubin, J. Basak, Y. Chetrit, H. Nguyen, R. Cohen, N. Izhaky, and M. Paniccia, *Electron. Lett.* 23, 1196 (**2007**).
36. M. R. Watts, D. C. Trotter, R. W. Young, and A. L. Lentine, *Proc. 5th IEEE International Conference on Group IV Photonics* (**2008**), pp. 4–6.
37. Q. Xu, B. Schmidt, S. Pradhan, and M. Lipson, *Nature* 435, 325 (**2005**).
38. L. Zhou and A. W. Poon, *Opt. Express* 14, 6851 (**2006**).

39. Q. Xu, B. Schmidt, J. Shakya, and M. Lipson, *Opt. Express* 15, 430 **(2007)**.
40. W. M. J. Green, M. J. Rooks, L. Sekaric, and Y. A. Vlasov, *Opt. Express* 15, 17106 **(2007)**.
41. R. A. Soref and B. R. Bennett, *IEEE J. Quantum Electron.* 23, 123 **(1987)**.
42. J. Liu, M. Beals, A. Pomerene, S. Bernardis, R. Sun, J. Cheng, L. C. Kimerling, and J. Michel, *Nat. Photon.* 2, 433 **(2008)**.
43. Y. Kuo, H. Chen, and J. E. Bowers, *Opt. Express* 16, 9936 **(2008)**.
44. H. Chen, Y. Kuo, and J. E. Bowers, *Opt. Express* 16, 20571 **(2008)**.
45. B. E. Little, H. A. Haus, J. Foresi, L. C. Kimerling, E. P. Ippen, and D. J. Ripin, *IEEE Photon. Technol. Lett.* 10, 816 **(1998)**.
46. S. J. B. Yoo, *J. Lightwave Technol.* 14, 955 **(1996)**.
47. Y. Kuo, H. Rong, V. Sih, S. Xu, M. Paniccia, and O. Cohen, *Opt. Express* 14, 11721 **(2006)**.
48. Q. Xu, V. R. Almeida, and M. Lipson, *Opt. Lett.* 30, 2733 **(2005)**.
49. A. C. Turner, M. A. Foster, A. L. Gaeta, and M. Lipson, *Opt. Express* 16, 4881 **(2008)**.
50. P. Dumon, G. R. A. Priem, L. R. Nunes, W. Bogaerts, D. Van Thourhout, P. Bienstman, T. K. Liang, M. Tsuchiya, P. Jaenen, S. Beckx, J. Wouters, and R. Baets, *Jpn. J. Appl. Phys.* 45, 6589 **(2006)**.
51. P. G. Kik, A. Polman, S. Libertino, and S. Coffa, *J. Lightwave Technol.* 20, 834 **(2002)**.
52. J. D. B. Bradley, P. E. Jessop, and A. P. Knights, *Appl. Phys. Lett.* 86, 241103 **(2005)**.
53. T. K. Liang, H. K. Tsang, I. E. Day, J. Drake, A. P. Knights, and M. Asghari, *Appl. Phys. Lett.* 81, 1323 **(2002)**.
54. J. Brouckaert, G. Roelkens, D. Van Thourhout, and R. Baets, *IEEE Photon. Technol. Lett.* 19, 1484 **(2007)**.

Received: 30 December 2008. Accepted: 31 March 2009.